

Influence of the upper critical field anisotropy on the transport properties of polycrystalline MgB₂

M. Eisterer,^{1,*} C. Krutzler,¹ and H. W. Weber¹

¹*Atominstitut der Österreichischen Universitäten, 1020 Vienna, Austria*

(Dated: March 23, 2022)

The intrinsic properties of MgB₂ form the basis for all applications of this superconductor. We wish to emphasize that the application range of polycrystalline MgB₂ is limited by the upper critical field H_{c2} and its anisotropy. In wires or tapes, the MgB₂ grains are randomly oriented or only slightly textured and the anisotropy of the upper critical field leads to different transport properties in different grains, if a magnetic field is applied and the current transport becomes percolative. The irreversibility line is caused by the disappearance of a continuous superconducting current path and not by depinning as in high temperature superconductors. Based on a percolation model, we demonstrate how changes of the upper critical field and its anisotropy and how changes of flux pinning will influence the critical currents of a wire or a tape. These predictions are compared to results of neutron irradiation experiments, where these parameters were changed systematically.

PACS numbers: 74.70.Ad, 74.81.Bd, 74.25.Sv, 64.60.Ak

INTRODUCTION

The strong field dependence of the critical current densities in MgB₂ represents one of the major problems for power applications of this material, where a current density of at least 10^8 A/m² is needed. Such high current densities can be obtained in conventional superconductors up to fields close to the upper critical field. In high temperature superconductors thermally activated depinning limits high current densities to relatively small magnetic fields compared to the huge upper critical fields of these materials. In MgB₂ thermal effects should play only a minor role due to its comparatively low Ginzburg number. Nevertheless, the critical currents become too small for power applications at fields well below H_{c2} , even at 4.2 K. Fortunately, the upper critical field of MgB₂ can be rather easily enhanced by certain preparation conditions [1, 2, 3], doping [4, 5, 6, 7, 8] or irradiation [9, 10, 11], and exceeds 30 T (at 0 K). Even for such "high- H_{c2} " materials, the application range is limited to around 10 T in polycrystalline samples. It was pointed out recently [12] that this small application range was caused by the upper critical field anisotropy of MgB₂. In the pure material, B_{c2} is about 14 T, if the field is applied parallel to the boron planes, while it is smaller than 3 T, if the field is applied perpendicular to the boron planes, leading to an anisotropy of close to 5 [13, 14, 15, 16, 17, 18]. In polycrystalline MgB₂, the grains are randomly oriented and the first grains become normal conducting at B_{c2}^{\perp} , which is a few times smaller than the upper critical field of the whole sample (B_{c2}^{\parallel}), thus reducing the effective cross section and the critical current of the conductor. In this paper the influence of the anisotropy will be discussed quantitatively. We will demonstrate that B_{c2}^{\perp} is most important for the application range of MgB₂.

DISTRIBUTION OF THE UPPER CRITICAL FIELD

The material is assumed to be perfectly homogeneous, i.e. all grains are supposed to have identical intrinsic properties. B_{c2} of each grain depends only on its orientation to the applied field and can be calculated within anisotropic Ginzburg Landau theory [19]:

$$B_{c2}(\theta) = \frac{B_{c2}^{\parallel}}{\sqrt{\gamma^2 \cos^2(\theta) + \sin^2(\theta)}} \quad (1)$$

γ denotes the anisotropy factor of the upper critical field, i.e. $B_{c2}^{\parallel}/B_{c2}^{\perp}$, and θ is the angle between the applied field and the c-axis. This relation was found to be a good approximation for MgB₂ by torque measurements [14, 15], although deviations by a few percent were reported [20]. For a given angular distribution of the grains, the distribution of B_{c2} can be easily calculated from Equ. 1. In untextured MgB₂, the grains are randomly oriented (each crystallographic direction is equally distributed over the elements of the steradian $d\Omega = \sin\theta d\theta d\phi$) and their angles θ with respect to any direction are distributed as $\sin\theta$. Assuming B_{c2}^{\parallel} to be 14 T and the anisotropy γ to be 4.5, as in the pure material, the distribution of Fig. 1 is obtained. Unfortunately, more grains have a comparatively low B_{c2} . The material can *now* be considered as inhomogeneous, since the grains have different upper critical fields, depending on their orientation to the applied field. This field induced inhomogeneity can be observed by the broadening of the resistive transition in magnetic fields (Fig. 2). At zero field, where the upper critical field plays no role, the transition of the filament of an iron sheathed wire [21] is sharp and its width (0.7 K) not much larger than the transition width (0.3 K) of a single crystal. At higher fields, the anisotropy significantly broadens the transition of the wire (7.5 K) compared to

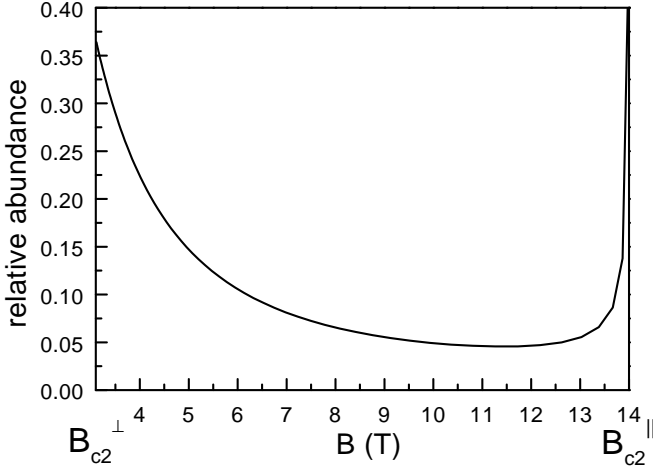


FIG. 1: Distribution of the upper critical field within the grains

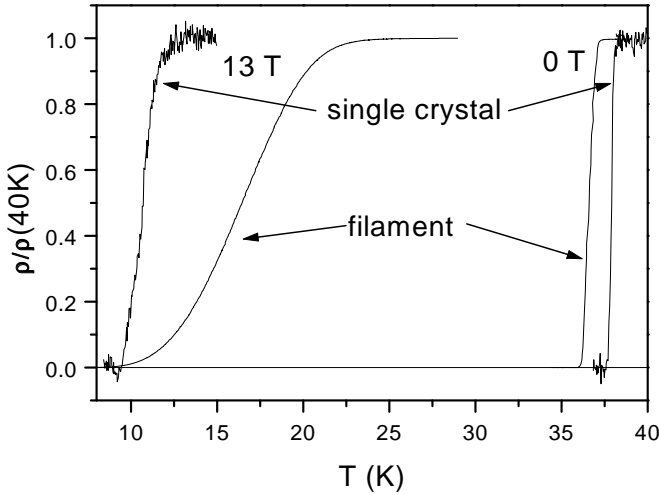


FIG. 2: Resistive transition of a polycrystalline sample ("filament") and of a single crystal ($H||ab$). The applied current density was in both specimens about 10^5 A/m².

the single crystal (1.8 K).

RESISTIVE TRANSITION

If a polycrystalline sample is cooled in a fixed applied field B_0 , the resistivity starts to deviate from its normal conducting behavior, when the first grains become superconducting. B_{c2} is defined by this onset of the transition and, therefore, B_0 corresponds to B_{c2}^{\parallel} at the actual temperature T^{on} . With decreasing temperature more and more grains become superconducting and the resistivity decreases. A grain becomes superconducting, if its upper critical field at the actual temperature becomes larger than the applied field. For a continuous superconducting current path, a certain fraction of the grains has to

be superconducting. This fraction is called percolation threshold or critical probability p_c and depends on the number of connections between the grains (coordination number). Percolation theory predicts a lower limit for p_c of about 0.162 for an irregular lattice [22] ("Finney pack") with a coordination number of 14.3. If the coordination number is only 6, p_c is calculated to be about 0.31 for a three dimensional lattice. These values correspond to the site percolation problem, which is the appropriate model for MgB_2 , since the nodes (grains in the real system) are switched on or off in site percolation problems, while the bonds between the nodes (grain boundaries) are switched in bond percolation problems. The fraction of superconducting grains p at a field B_0 , can be calculated by integration of the distribution function:

$$p = \int_{\theta_{min}}^{\frac{\pi}{2}} \sin \theta d\theta = \cos \theta_{min} \quad (2)$$

In the transition region θ_{min} is defined by $B_{c2}(\theta_{min}) = B_0$. Inserting relation 2 with $p = p_c$ into Equ. 1 leads to the field of zero resistivity

$$B_{\rho=0}(T) = \frac{B_{c2}^{\parallel}(T)}{\sqrt{(\gamma^2 - 1)p_c^2 + 1}} \quad (3)$$

The field, where the resistivity disappears, is commonly denoted as the irreversibility field. Since the finite resistivity in MgB_2 above $B_{\rho=0}$ is caused by a completely different mechanism than in high temperature superconductors, this field is denoted as "zero resistivity field" in the following. According to Equ. 3 the zero resistivity field is proportional to the upper critical field, as observed in experiments (Fig. 3). The symbols represent experimental data obtained on the filament of an iron sheathed wire. The onset and the offset of the transition were defined by 90 % and by 10 % of the resistivity at 40 K, respectively. The line graph was calculated with $\gamma = 4.5$ and $p_c = 0.25$.

At fixed applied field the condition for the offset of the transition becomes $B_{\rho=0}(T^{off}) = B_0$ and - assuming only B_{c2}^{\parallel} to be temperature dependent - the transition width $\Delta T := T^{on} - T^{off}$ is obtained as [12]

$$\Delta T = \frac{\sqrt{(\gamma^2 - 1)p_c^2 + 1} - 1}{(-\frac{\partial B_{c2}}{\partial T})} B_0 \quad (4)$$

The transition width is predicted to decrease with decreasing anisotropy γ . This can be demonstrated by neutron irradiation experiments. Neutron irradiation increases the upper critical field of MgB_2 and decreases its anisotropy [23, 24]. The resistive transition of a sintered MgB_2 sample is plotted in Fig. 4 before and after neutron irradiation. The shift of B_{c2} and the predicted decrease of the transition width can be observed.

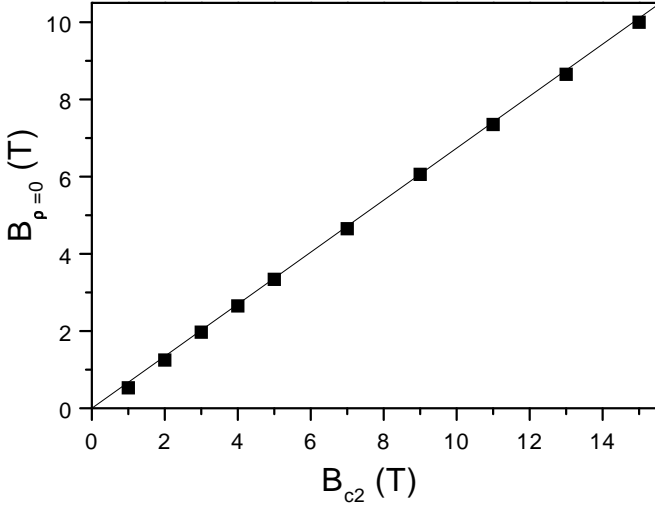


FIG. 3: Zero resistivity field as a function of the upper critical field. Symbols refer to experimental data, the line represents the expected behavior for $\gamma=4.5$ and $p_c=0.25$.

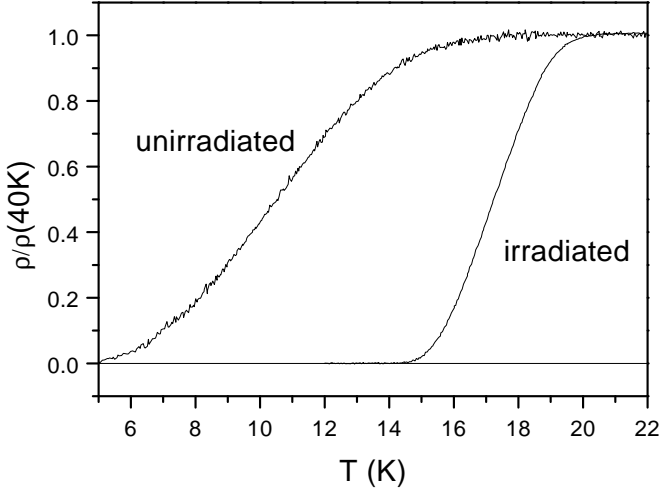


FIG. 4: Resistive transition at 13 T before and after neutron irradiation.

In our considerations we neglect the influence of sample inhomogeneities and of thermal activation of the flux lines. Both effects would additionally increase the transition width. Inhomogeneities shift the transitions of equally oriented grains and thermally activated depinning broadens the transition of each individual grain, but is assumed to be zero (cf. the transition of the single crystal in Fig. 2). However, in reasonably homogeneous samples, the anisotropy is the dominant parameter, since it predicts the correct magnitude of the transition width (except for low magnetic fields). The transition width calculated from Equ. 4 represents a lower limit and is close to typical experimental data under realistic assumptions for p_c and for γ , not leaving much room for additional effects. On the other hand, a conducting

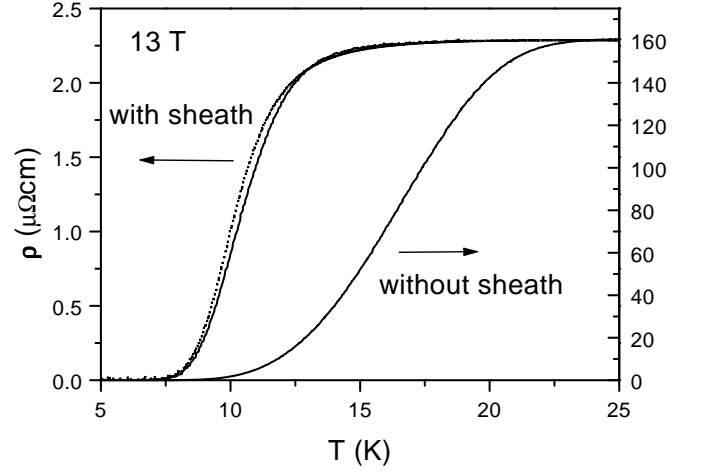


FIG. 5: Resistive transition of a wire before and after removing the conducting sheath

sheath can decrease the experimental transition width significantly, as shown in Fig. 5. The iron sheath of a wire with a total diameter of 1.1 mm was removed by etching, the remaining filament had a diameter of about 0.65 mm. The resistivity increased by nearly two orders of magnitude from about $2.28 \mu\Omega\text{cm}$ to about $160 \mu\Omega\text{cm}$. The onset of the transition (defined by the 90 % criterion) was shifted from 12.7 K to 20 K and the transition width increased from 3.8 K to 7.5 K. These changes are mainly due to the removal of the parallel resistivity of the iron sheath, since the original curve can be recalculated by assuming a parallel resistivity of $2.32 \mu\Omega\text{cm}$ (dotted curve in Fig. 5). The small difference can be explained by the resistivity between the iron sheath and the filament and/or by small property changes due to the strain exerted by the iron sheath [25]. For the analysis of the anisotropy, the *real* B_{c2} and $B_{\rho=0}$ are needed, which can only be determined after removing the conducting sheath.

CRITICAL CURRENTS

From the distribution of the upper critical fields (cf. Fig. 1) the distribution of the critical current densities within the grains can be obtained, if a certain pinning model is assumed. For grain boundary pinning, J_c is related to B_{c2} via [26]

$$J_c(\theta) = J_{c0} \frac{(1 - B/B_{c2}(\theta))^2}{\sqrt{B_{c2}(\theta)B}} \quad (5)$$

for $B < B_{c2}$ and $J_c = 0$ otherwise. The coefficient J_{c0} represents the pinning strength. J_c of a polycrystalline sample can be calculated from the distribution of the critical current densities [12] within the framework of percolation theory. This is demonstrated in Fig. 6 for

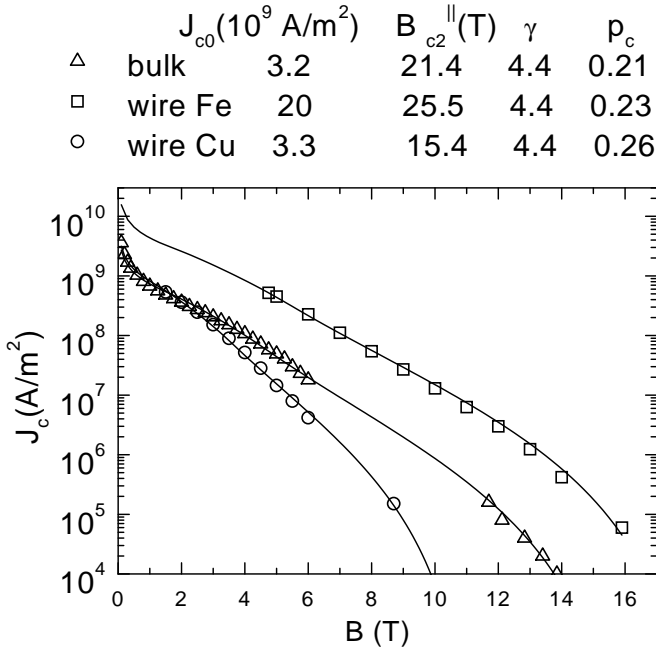


FIG. 6: Critical current densities of a bulk sample at 5 K and of two different wires at 4.2 K.

different samples, i.e. a sintered bulk material, a copper sheathed in-situ wire [27] and an iron sheathed in-situ wire [21]. The experimental data (symbols in Fig. 6) were obtained by direct transport measurements (using a $1 \mu\text{V}/\text{cm}$ criterion) in the case of the wires, and by ac measurements [28] on the bulk sample. For the calculation of J_c (lines in Fig. 6) four parameters are needed. The upper critical field B_{c2} of the sample (i.e. B_{c2}^{\parallel} of the grains), the anisotropy γ , the percolation threshold p_c and the pinning strength J_{c0} . While B_{c2} was measured directly at high temperatures and extrapolated to low temperatures, the other parameters have to be fitted to the experimental data. The critical current densities can be well described by the same anisotropy for all three samples and similar values for the percolation threshold. The pinning strength of the Cu-sheathed wire and the bulk sample is nearly identical, the smaller field dependence of J_c in the bulk sample is caused by its higher B_{c2} . The iron sheathed wire has the largest upper critical field and shows the strongest pinning, which leads to the highest current densities at all fields.

The primary influence of neutron irradiation in MgB_2 lies in the increase of B_{c2} and the decrease of anisotropy. Nearly no changes of J_c at low fields, but a strong enhancement of J_c at high magnetic fields are observed (Fig. 7). The upper critical field increases from 21.4 T and 15.4 T to 30 T and 18.6 T, respectively, the anisotropy γ (obtained from fitting) decreased from about 4.4 in both samples to 2.8 and 2.6 in the bulk and in the copper sheathed wire, respectively. This decrease of γ is consistent with direct measurements of the

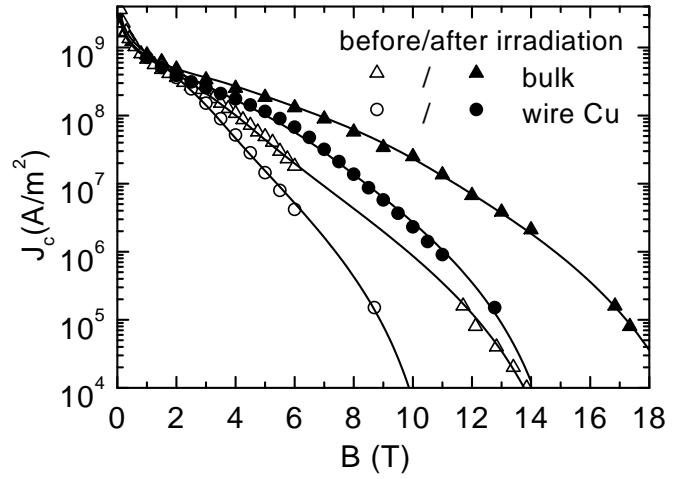


FIG. 7: Critical current densities before and after neutron irradiation.

upper critical field anisotropy in single crystals [23, 24]. The influence on pinning is rather small. The increase of B_{c2} reduces the pinning strength [26] ($J_c \propto 1/\sqrt{B_{c2}}$), but J_{c0} of the sintered bulk sample increases by 25 % after irradiation, which can be attributed to the introduction of pinning centers, as observed in single crystals [29]. These competing effects lead to an increase of the pinning strength by only about 5 % at low magnetic fields. The pinning strength even decreases by about 10 % in the wire. Therefore, the enhancement of J_c after neutron irradiation is caused mainly by changes in the reversible parameters of MgB_2 . Since these changes of the reversible parameters were observed independently on single crystals, the percolation model [12] correctly predicts the changes of the critical currents in polycrystalline samples.

CONSEQUENCES/STRATEGY

Based on the quantitative agreement between anisotropy-induced percolation theory and experimental data on polycrystalline MgB_2 , the fundamental parameters of this theory can be exploited for an assessment of their individual impact on the current carrying capability of MgB_2 . We will, therefore, systematically investigate the influence of variations in its four parameters. $J_c(B)$ calculated from the parameters of the iron sheathed wire will be used as reference (dotted line in Fig. 8) and only one parameter will be changed by 30 % in each scenario. The critical current density of the wire drops to 2×10^8 A/m² (horizontal lines in Fig. 8), which is a reasonable limit for power applications and defines the application range in the subsequent investigation, very closely to the upper critical field $B_{c2}^{\perp} = 5.8$ T (vertical lines in Fig. 8).

The first strategy is an improvement of pinning. This can be achieved by the addition of pinning centers or,

in the case of grain boundary pinning, by a very fine grain structure. If the corresponding parameter, J_{c0} , is increased, the critical current densities are enhanced at all fields by the same factor (Fig. 8a). Although this is favorable at low magnetic fields, it has little effect on the application range. The simple shift (on a logarithmic scale) of $J_c(B)$ to higher values only occurs, if the pinning mechanism remains unchanged, i.e. the critical current densities of the individual grains can be described by Equ. 5. However, since J_c becomes zero at B_{c2} for any pinning mechanism, the strong field dependence and the importance of B_{c2}^\perp cannot be changed qualitatively by different pinning centres.

As a second strategy, an increase of the upper critical field is considered. It is well documented that B_{c2} can be enhanced significantly by various techniques [1, 2, 3, 4, 5, 6, 7, 8, 9, 10, 11]. Although the mechanisms involved in these changes are not yet fully understood, impurity scattering in both bands seems to play a major role. However, there must be a mechanism, which enhances B_{c2}^\parallel without significantly changing γ (cf. Fig. 6). A shift of the upper critical field from 25.5 T to 33.15 T results in a strong increase of the zero resistivity field and in higher critical currents at high magnetic fields (Fig. 8b). Since the anisotropy is constant, B_{c2}^\perp increases to 7.5 T. J_c falls below 2×10^8 A/m² exactly at B_{c2}^\perp .

A smaller percolation threshold p_c is the third possibility to improve the current carrying capability of polycrystalline MgB₂. This can be achieved by a homogeneous sample with a high density. Pores and normal conducting grains (e.g. MgO) increase p_c . A small percolation threshold enhances the zero resistivity field, but has no influence on J_c within the application range (Fig. 8c). In principle the density of the sample also affects J_{c0} due to the reduction of the superconducting cross section, but this effect is small in samples of good quality. For the present parameters, an increase of J_{c0} by about 15 % is expected. Since a p_c of 0.16 corresponds to the theoretical limit [22], a significant improvement of the transport properties cannot be expected from the optimization of p_c .

The last strategy is a reduction of the anisotropy γ . A reduction of γ was reported after neutron irradiation [23, 24] or can be achieved by carbon doping [30], but it seems to be always accompanied by an increase of the upper critical field B_{c2}^\parallel (which further enhances B_{c2}^\perp and enlarges the application range). Although experimentally difficult, the influence of such a "pure" change of anisotropy on J_c is demonstrated in Fig. 8d. γ is reduced from 4.4 to 3.1 or, equivalently, B_{c2}^\perp is increased by 2.4 T (from 5.8 T to 8.2 T). This also enlarges the application range by about 2 T and emphasizes again the importance of B_{c2}^\perp for power applications of MgB₂ in magnetic fields.

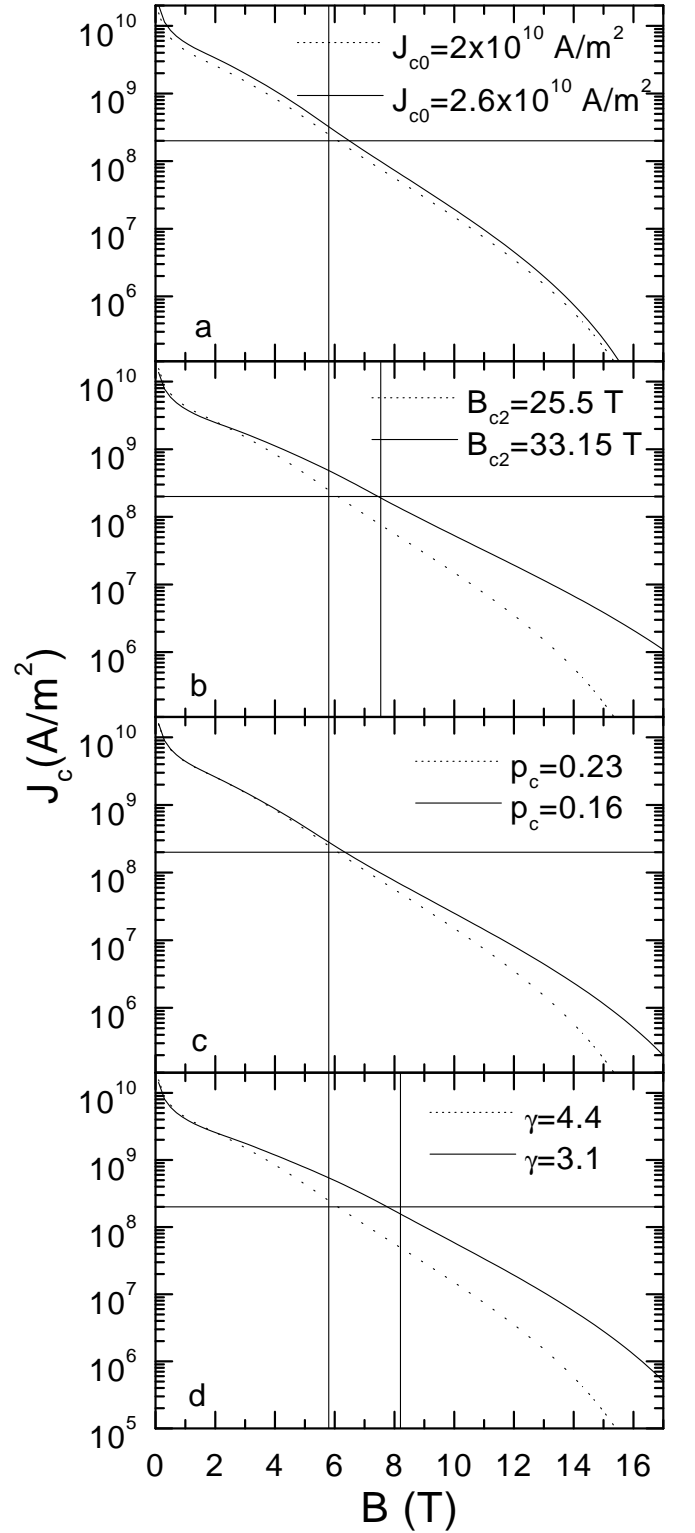


FIG. 8: Influence of various parameters on J_c . Only one parameter of the original data set (dotted curve) is changed in each panel.

CONCLUSIONS

The upper critical field and its anisotropy are the most important and determining for the field of zero resistivity in polycrystalline MgB_2 , in contrast to high temperature superconductors, where the irreversibility field is related to the pinning properties. The maximum magnetic field for power applications of MgB_2 is always close to B_{c2}^\perp . It is, therefore, essential to enhance B_{c2}^\perp for applications of MgB_2 at high magnetic fields.

We wish to thank Sonja Schlacher and Wilfried Goldacker from the Forschungszentrum Karlsruhe for providing us with the iron sheathed wire.

* Electronic address: eisterer@ati.ac.at

- [1] Y. Takano, H. Takeya, H. Fujii, H. Kumakura, T. Hatano, K. Togano, H. Kito, H. Ihara, *Appl. Phys. Lett.* **78**, 2914 (2001).
- [2] R. Flükiger, P. Lezza, C. Beneduce, N. Musolino, H. L. Suo, *Supercond. Sci. Technol.* **16**, 264 (2003).
- [3] A. Gurevich, S. Patnaik, V. Braccini, K.H. Kim, C. Mielke, X. Song, L.D Cooley, S.D. Bu, D.M. Kim, J.H. Choi, L.J. Belenky, J. Giencke, M.K. Lee, W. Tian, X.Q. Pan, A. Siri, E.E. Hellstrom, C.B. Eom, D.C. Larbalestier, *Supercond. Sci. Technol.* **17**, 278 (2004).
- [4] R.A. Ribeiro, S.L. Bud'ko, C. Petrovic, P.C. Canfield, *Physica C* **384**, 227 (2003).
- [5] S.X. Dou, V. Braccini, S. Soltanian, R. Klie, Y. Zhu, S. Li, X.L. Wang, D. Larbalestier, *J. Appl. Phys.* **96**, 7549 (2004).
- [6] R.H.T. Wilke, S.L. Bud'ko, P.C. Canfield, D.K. Finnemore, R.J. Suplinskas, S.T. Hannahs, *Phys. Rev. Lett.* **92**, 217003 (2004).
- [7] S.M. Kazakov, R. Puzniak, K. Rogacki, A.V. Mironov, N.D. Zhigadlo, J. Jun, Ch. Soltmann, B. Batlogg, J. Karpinski, *Phys. Rev. B* **71**, 024533 (2005).
- [8] M.D. Sumption, M. Bhatia, M. Rindfleisch, M. Tomsic, S. Soltanian, S. X. Dou, E. W. Collings, *Appl. Phys. Lett.* **86**, 092507 (2005).
- [9] M. Eisterer, M. Zehetmayer, S. Tönies, H.W. Weber, M. Kambara, N.H. Babu, D.A. Cardwell, L.R. Greenwood, *Supercond. Sci. Technol.* **15**, L9 (2002).
- [10] Y. Wang, F. Bouquet, I. Sheikin, P. Toulemonde, B. Revaz, M. Eisterer, H.W. Weber, J. Hinderer, A. Junod, *J. Phys.: Condens. Matter* **15**, 883 (2003).
- [11] M. Putti, V. Braccini, C. Ferdeghini, F. Gatti, G. Grasso, P. Manfrinetti, D. Marré, A. Palenzona, I. Pallecchi, C. Tarantini, I. Sheikin, H. U. Aebersold, E. Lehmann, *Appl. Phys. Lett.* **86**, 112503 (2005).
- [12] M. Eisterer, M. Zehetmayer, H.W. Weber *Phys. Rev. Lett.* **90**, 247002 (2003).
- [13] Y. Eltsev, S. Lee, K. Nakao, N. Chikumoto, S. Tajima, N. Koshizuka, M. Murakami, *Phys. Rev. B* **65**, 140501 (2002).
- [14] M. Angst, R. Puzniak, A. Wisniewski, J. Jun, S. M. Kazakov, J. Karpinski, J. Roos, H. Keller, *Phys. Rev. Lett.* **88**, 167004 (2002).
- [15] M. Zehetmayer, M. Eisterer, J. Jun, S. M. Kazakov, J. Karpinski, A. Wisniewski, H.W. Weber, *Phys. Rev. B* **66**, 052505 (2002).
- [16] A. V. Sologubenko, J. Jun, S. M. Kazakov, J. Karpinski, H.R. Ott, *Phys. Rev. B* **65**, 180505 (2002).
- [17] L. Lyard, P. Samuely, P. Szabo, T. Klein, C. Marcenat, L. Paulius, K.H.P. Kim, C.U. Jung, H.-S. Lee, B. Kang, S. Choi, S.-I. Lee, J. Marcus, S. Blanchard, A.G. M. Jansen, U. Welp, G. Karapetrov, W.K. Kwok, *Phys. Rev. B* **66**, 180502 (2002).
- [18] U. Welp, A. Rydh, G. Karapetrov, W.K. Kwok, G.W. Crabtree, C. Marcenat, L. Paulius, T. Klein, J. Marcus, K.H.P. Kim, C.U. Jung, H.-S. Lee, B. Kang, S.-I. Lee, *Phys. Rev. B* **67**, 012505 (2003).
- [19] D. R. Tilley, *Proc. Phys. Soc. (London)* **86**, 289 (1965).
- [20] A. Rydh, U. Welp, A.E. Koshelev, W.K. Kwok, G.W. Crabtree, R. Brusetti, L. Lyard, T. Klein, C. Marcenat, B. Kang, K.H. Kim, K.H.P. Kim, H.-S. Lee, S.-I. Lee, *Phys. Rev. B* **70**, 132503 (2004).
- [21] W. Goldacker, S.I. Schlachter, B. Obst, B. Liu, J. Reiner, S. Zimmer, *Supercond. Sci. Technol.* **17**, S363 (2004).
- [22] S. C. van der Marck, *Phys. Rev. E* **55**, 1514 (1997).
- [23] M. Zehetmayer, M. Eisterer, J. Jun, S. M. Kazakov, J. Karpinski, H.W. Weber, *Phys. Rev. B* **70**, 214516 (2004).
- [24] M. Eisterer, *phys. stat. sol. (c)* **2**, **5**, 1606 (2005).
- [25] P. Kovac, M. Dhallé, T. Melisek, H.J.N. van Eck, W.A.J. Wessel, B. ten Haken, I. Husek, *Supercond. Sci. Technol.* **16**, 600 (2003).
- [26] D. Dew-Hughes, *Phil. Mag.* **30**, 293 (1974).
- [27] B.A. Glowacki, M. Majoros, M. Vickers, J.E. Evetts, Y. Shi, I. McDougall, *Supercond. Sci. Technol.* **14**, 193 (2001).
- [28] M. Eisterer, H.W. Weber, *J. Appl. Phys.* **88**, 4749 (2000).
- [29] M. Zehetmayer, M. Eisterer, J. Jun, S. M. Kazakov, J. Karpinski, B. Birajdar, O. Eibl, and H. W. Weber, *Phys. Rev. B* **69**, 054510 (2004).
- [30] T. Masui, S. Lee, S. Tajima, *Phys. Rev. B* **70**, 024504 (2004).